Thermosensitive poly(N-isopropylacrylamide) based cryogel: A SAXS study

Isıya duyarlı poli(N-izopropilakrilamit) temelli kriyojellerin SAXS çalışması

Review Article

Veyis Karakoç[1], Elif Hilal Şen[2], Semra İde[3], Deniz Türkmen[1], Rabel Soomro[4], Adil Denizli[1]*

[1] Department of Chemistry, Biochemistry Division, Hacettepe University, Ankara, Turkey
[2] Faculty of Science, Department of Physics, Karadeniz Technical University, Trabzon, Turkey
[3] Department of Physics Engineering, Hacettepe University, Ankara, Turkey
[4] National Centre of Excellence in Analytical Chemistry, University of Sindh, Jamshoro, Pakistan

ABSTRACT

The purpose of this study is to observe the structural changes of the thermosensitive poly(N-isopropylacrylamide-N-methacryloyl-L-histidine) poly(NIPA-MAH) monolithic cryogel with changing temperature around lower critical solution temperature (LCST) of NIPA by Small Angle X-Ray Scattering (SAXS). Poly(NIPA-MAH) cryogel was prepared by free radical cryocopolymerization of NIPA with MAH as functional comonomer and N,N-methylene-bisacrylamide (MBAAm) as crosslinker directly in a plastic syringe. Polymerization initiated by N,N,N,N-tetramethylene diamine (TEMED) and ammonium persulfate (APS) pair at subzero temperature in an ice bath. LCST of poly(NIPA-MAH) cryogel was found to be 34°C. Poly(NIPA-MAH) cryogel with 60–100 μm in pore diameter have a specific surface area of 42.6 m^2/g polymer. This porous cryogel form provides fast temperature response comparing to conventional gels. The surface morphology and bulk structure of poly(NIPA-MAH) cryogel revealed with scanning electron microscopy (SEM). SAXS allowed the determination of nanoalteration of poly(NIPA-MAH) cryogel such as pore volume, wall thickness and pore shape with changing temperature. Scattering data were analysed both native form and in water at temperature range of 30°C-40°C. At two different temperatures 34°C and 35°C a detailed investigation on shape of pores and pore size; which indicating a recordable change, were also carried out.

Key words

N-isopropylacrylamide (NIPA), thermosensitive, cryogels, Small Angle X-Ray Scattering (SAXS)

ÖZET

Bu çalışmanın amacı, NIPA'in düşük kritik çözelti sıcaklığı (LCST) civarındaki sıcaklığın değiştirilmesiyle ısıya duyarlı poli(N-izopropilakrilamid-metakriloil-L-histidin), poli(NIPA-MAH) monolitik kriyojellerinin nano yapısındaki değişimleri küçük açı x-ışını saçılması (SAXS) yöntemi ile incelemektir. Poli(NIPA-MAH) kriyojeller, NIPA, MAH fonksiyonel monomeri ve N,N-metilen-bisakrilamit (MBAAm) çapraz bağlayıcısı kullanılarak plastik şırınga içerisinde serbest radikal kriyopolimerizasyonu ile hazırlanmıştır. Polimerizasyon buz banyosunda sıfır derecenin altında N, N, N, N-tetrametilen diamin (TEMED) ve amonyum persulfat (APS) çifti kullanılarak başlatılmıştır. Poli(NIPA-MAH) kriyojelinin LCST değeri 34 °C olarak bulunmuştur. Poli(NIPA-MAH) kriyojelleri 60-100 μm gözenek çapına ve 42.6 m^2/g polimer spesifik yüzey alanına sahiptir. Sentezlenen gözenekli kriyojeller geleneksel jellerle karşılaştırıldığında sıcaklık değişimine hızlı tepki vermektedir. Poli(NIPA-MAH) kriyojelinin yığın yapısı ve yüzey morfolojisi taramalı elektron mikroskobu (SEM) kullanılarak belirlenmiştir. SAXS, poli(NIPA-MAH) kriyojelinin sıcaklık değişimiyle gözenek hacmi, duvar kalınlığı ve gözenek şekli gibi nano boyuttaki değişimlerin belirlenmesine imkan vermektedir. 30-40°C sıcaklık aralığında doğal form ve su içerisinde saçılma verileri incelenmiştir. Iki farklı sıcaklıkta (34°C ve 35°C) gözenek boyutu ve şekli üzerinde kaydedilebilir bir değişikliği gösteren ayrıntılı bir inceleme de gerçekleştirilmiştir.

Anahtar Kelimeler

N-izopropilakrilamid (NIPA), ısıl duyarlı, kriyojel, Küçük Açı X-ışını Saçılması (SAXS)

Article History: Received: Nov 18, 2013; Revised: Dec 25, 2014; Accepted: Feb 11, 2014; Available Online: Jun 30, 2014.

Corresponding author: A. Denizli, Hacettepe University, Department of Chemistry, Biochemistry Division, Beytepe, 06800, Ankara, Turkey

Tel: +903122977963 Fax: +90312 299 2163 E-Mail: denizli@hacettepe.edu.tr

INTRODUCTION

Intelligent gels which change their volume and pyhsical features such as surface properties as a result of slight variation of external stimule such as temperature, pH, ionic strength, etc. [1,2]. Thermosensitive gels, that member of the intelligent gels, have attracted a great deal of attention for the applications to drug delivery, enzyme immobilization, actuators, separation of biomolecules and removal of toxic materials and metals [3-8]. NIPA is a well known and most studied thermosensitive polymer with a Lower Critical Solution Temperature (LCST) of around 32°C. NIPA is hydrophilic and has swollen form in water below 32°C and it shrunks sharply and become hydrophobic when the temperature above 32°C [9]. The LCST value of NIPA is close to the physiological temperature, due to the unique properties of NIPA have been widely used in biomedicine, biomaterial and biotechnological fields including purification and separation of biomolecules [10-13]. The LCST of NIPA can be changed using hydrophobic or hydrophilic monomers.

Macroporous gels obtained at temperatures below the freezing point of solvent are called cryogels [14]. Cryogels have interconnected pores and sponge like morphology. Cryogels have macropores which in sizes of 10 -100 μm. Highly porous structure and sufficiently large pore size provides non hindered diffusion in the gels for all solutes including macromolecules and convective transport of viscous media [15]. Porous cryogel is also used to capture and separate target biomolecules with direct application of crude cell homogenates, solid particulates such as microbial cells or cell debris in the culture fluids and bioproducts such as recombinant proteins, enzymes, cells and viruses in downstream processes [16]. The unique macroporous morphology of cryogels makes them attractive matrixes for chromatography. The other advantage of the porous cryogel is very short swelling/shrinkage time with respect to the conventional gel of the same chemical composition [17-20].

For several biotechnological applications, NIPA may require modification without losing the thermosensitivity. Amino acid molecules have been used as pseudo-affinity ligands since they are resistant to harsh chemicals and high temperatures as well as their low cost, with high biocompatibility [26]. Histidine have greater affinity for IgG. In the literature histidine affinity ligand has been used for IgG purification [27]. Histidine has imidazole ring which led to electrostatic interactions between imidazole group and IgG besides changing surface property of NIPA by adjusting temperature.

In this study, MAH used as comonomer in order to obtain responses to multiple external stimuli, such as temperature and there is no significant loss of the thermosensitivity of NIPA cryogels. The alteration of surface properties from hydrophilic to hydrophobic character in thermosensitive poly(NIPA-MAH) was investigated by Small Angle X-ray Scattering (SAXS). Literature also reports that SAXS is widely used to reveal the internal structure of the gels and other polymeric materials [28]. Especially in intelligent materials to reveal the alteration of pore volume and wall thickness of gels by changing environmental conditions such as temperature, there are many studies about the characterization of thermosensitive polymers [29-33].

EXPERIMENTAL

Materials

L-histidine, methacryloyl chloride, N,N-methylene-bis(acrylamide) (MBAAm), ammonium persulfate (APS) and wide range molecular weight marker were supplied by Sigma Chemical Co. (St Louis, MO). N-isopropylacrylamide (NIPA) was obtained from Aldrich Chem. Co. (USA) distilled under reduced pressure in the presence of hydroquinone inhibitor, and stored at 4°C until use. N,N,N,N-Tetramethylenethylene diamine (TEMED) was also obtained from Fluka A.G. All other chemicals used were reagent grade and obtained from Merck A.G. (Darmstadt, Germany) unless otherwise noted. All water used in the experiments was purified using a Barnstead

(Dubuque, IA) ROpure LP reverse osmosis unit with a high-flow cellulose acetate membrane (Barnstead D2731) followed by a Barnstead D3804 NANOpure organic/colloid removal and ion-exchange packed-bed system.

Synthesis of MAH monomer

Details of the preparation and characterization of N-methacryloyl-(L)-histidine (MAH) was reported elsewhere [34]. The following procedure was applied for the synthesis of MAH monomer: 5.0 g of L-histidine and 0.2 g of hydroquinone were dissolved in 100 ml of CH_2Cl_2 solution. Solution was cooled down to 0°C. 12.74 g of triethylamine was added to the solution. 5.0 ml of methacryloyl chloride was poured slowly into this solution under nitrogen atmosphere and then this solution was stirred magnetically at room temperature for 2 h. At the end of this chemical reaction period, unreacted methacryloyl chloride was extracted with 10% NaOH. Aqueous phase was evaporated in a rotary evaporator. The residue (i.e., MAH) was crystallized in ethanol and ethyl acetate.

Preparation of poly(NIPA-MAH) cryogel

Copolymer of N-isopropylacrylamide with MAH was synthesized by free radical cryopolymerization [33]. A typical preparation procedure is as follow: NIPA (300 mg) and MAH (200 mg) were dissolved in 5.0 mL deionized water. MBAAm (0.283 g) was dissolved in 10 mL deionized water and these solutions were mixed. After adding APS (1 % of the total monomers, w/v) the solution was cooled in an ice bath for 5 min. TEMED (1 % of the total monomers, w/v) was added and the reaction mixture was stirred for 1 min. Then, the reaction mixture was poured into a plastic syringe (total volume: 5 mL, internal diameter: 0.8 cm) with closed outlet at the bottom. The polymerization solution in the syringe was frozen at -16°C for 24 h. The frozen system consists of solid phase (crystals of frozen water) and unfrozen liquid monomer phase. During the freezing process the solvent (water in our case) is converted to ice crystals. Then, melting of ice crystals in frozen system leaves macropores in the gels at room temperature. After thawing, cryogel was washed with ethanol/water mixture 30/70 (v/v)to remove unreacted monomer and other impurities. The surface morphology of poly(NIPA-MAH) cryogel was examined using SEM. Firstly the sample was dehydrated at -50°C in lyophilizer (Lyophilizer, Christ Alpha 1-2 LD plus, Germany). Then, the sample was examined using a scanning electron microscope (JEOL JSM 5600, Tokyo, Japan).

SAXS studies

SAXS was used to investigate the molecular and nanosized structure of the poly(NIPA-MAH) cryogel. At room temperature, the nanostructures of dry and wet form of the sample were compared to define the highly porous property. SAXS scans were also carried out from 30°C to 40°C using an external temperature control unit with temperature increase by 1°C to investigate thermal effects on the structure of poly(NIPA-MAH) cryogel. Small Angle X-Ray Scattering (SAXS) profiles were recorded by a HECUS- SWAXS (Hecus X-Ray Systems, Graz, Austria) system including Kratky slit-optic, line collimation and an X-ray generator operating at 50 kV and 40 mA with Cu anode [λ(CuKα) = 1.54 Å] in q range of 0.008 – 1.22 ($Å^{-1}$). A small part of dry sample was measured at room temperature by using a convenient sample holder. The scattering intensity profiles were corrected for background scattering. In the thermal analysis of the sample, first measurement was done by a wet polymer (incubated in water during an hour) at room temperature to compare the scattering profile with that of dry sample. Then, the other thermal measurements were made by a step scanning procedure (in the temperature range of 30°C – 40°C and each increasing value of 1°C) and in fixed time mode, with a sampling time 900 s.

RESULTS AND DISCUSSION

Thermosensitive poly(NIPA-MAH) monolithic cryogel was produced by cryopolymerization in the frozen state of monomers, N-isopropylacrylamide (NIPA) and N-methacryloyl-(L)-histidine (MAH) with N,N-methylene-bis(acrylamide) (MBAAm) as

a cross-linker in the presence of TEMED/APS as initiator/accelerator pair. The poly(NIPA-MAH) monolithic cryogel was prepared successfully with opaque, sponge like and elastic form. The scanning electron micrographs of the poly(NIPA-MAH) cryogel were shown in Figure 1. The open and highly interconnected megapores can be seen clearly in the cryogel structure. The large pores allow transport of viscous samples such as, body fluids, blood, and plasma proteins, without any obstacle through the pores

A real material never completely fulfills the idealization stipulated in the ideal two phase model. Therefore some modifications have to be used to derive well suited theoretical expressions for the fitting process of the experimentally observed intensity data. These modifications must be related with density fluctuation within the phases and diffuse interface boundary [35]. The main theoretical expressions and approximations have been used for the scattering data of our studied cryogels [36]. But a well fitted equation of the x-ray scattering could not be obtained to reach the detailed structural parameters. However, the structural parameters mentioned below, were obtained with the basic SAXS analysis on our cryogels.

The SAXS intensity [I(q)] for porous structures can be given as the following formula:

$$I(q) = V\varphi_1\varphi_2(\Delta\rho)^2 \int_0^\infty 4\pi r^2 \gamma_0(r)\frac{sinqr}{qr}\, dr \quad (1)$$

where $q = 4\pi(\sin\theta/\lambda)$ is the magnitude of scattering vector, V is the scattering volume, ϕ_1 and ϕ_2 are the volume fractions of the polymer and pores, $\Delta\rho$ is the average electron density difference between two phases, $\gamma_0(r)$ is the correlation function.

The X-ray scattering power of the dry cryogel is bigger than that of the cryogel in water. Because of the electron densities of polymer regions is greater than that of water filled and stretched polymer borders and pores. So, the lower scattering intensity of wet cryogel has been obtained as expected in Figure 2.

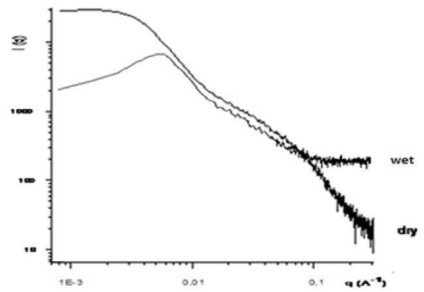

Figure 2. Scattering profiles of the dry and wet poly(NIPA-MAH) cryogel at 25ºC.

Pore sizes for these two cryogels in the form of dry and wet were evaluated by Guiner approximation (q→0) and the value of 11.4 nm (dry) and 15.4 nm (wet) were determined. This result is indicating bigger pore size in the wet form because of physical effect of the water

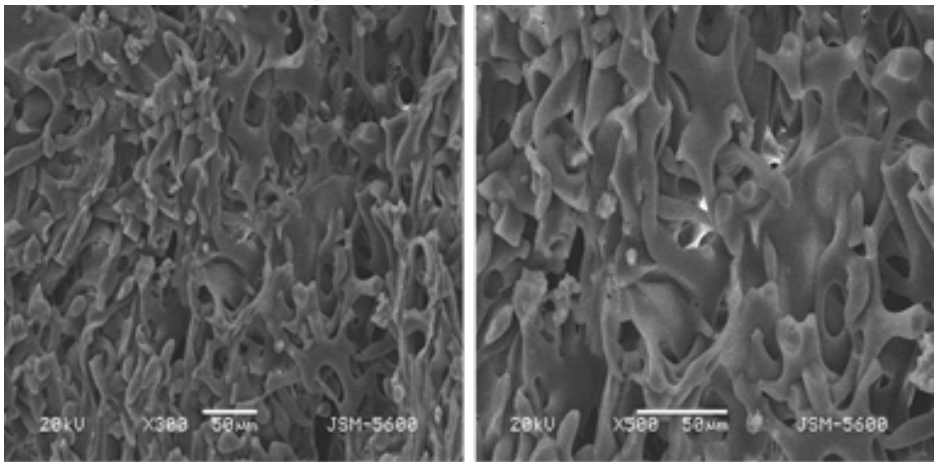

Figure 1. Scanning electron micrographs of the poly(NIPA-MAH) cryogel.

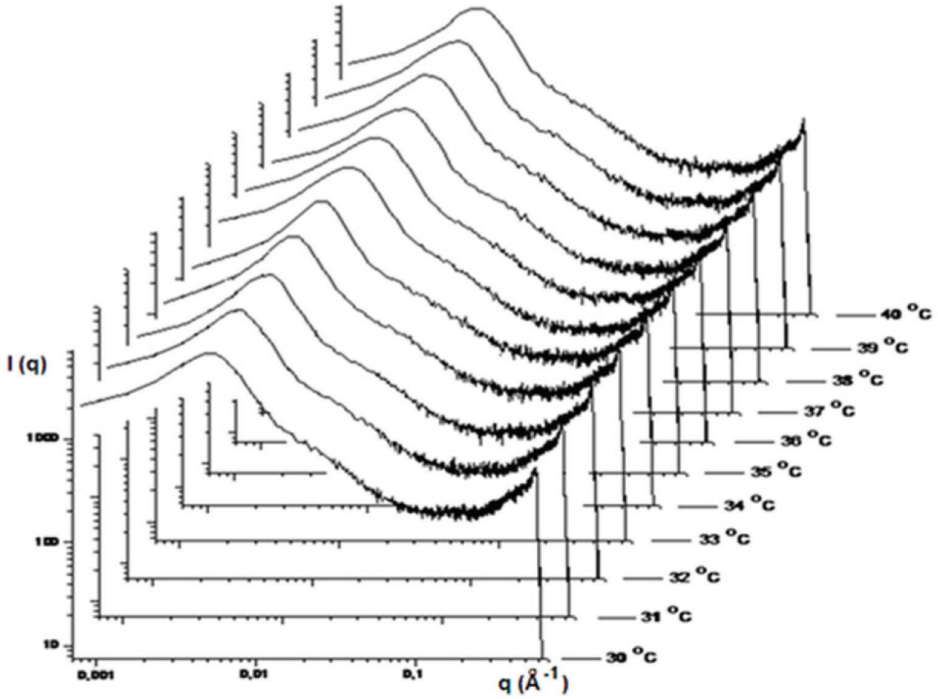

Figure 3. SAXS patterns of poly(NIPA-MAH) cryogels in the temperature range of 30-40 ºC.

filling. Fractal behaviour of the polymer borders is also effectively changing as seen in the bigger q range [in Porod region (q →∞)] of the scattering profile. This behaviour will be discussed in the following content.

Structural changes can be seen in the middle part (q: 0.01-0.1 $Å^{-1}$) of the scattering profiles given in Figure 3 while the radius of gyration graphic as a function of temperature can be followed in Figure 4.

The fluctuations within the radius of gyration values can be explained by water diffusion throughthe pores, increasing pore sizes with water up to a critical temperature, ripping of the stretched polymer borders, exploding the water filled pores and forming of new water channels. Then, the smallest pores are also started to fill with water and new pores filled water can be also formed by the shrinking polymer borders and close contacts after the ripping with temperature increase. With the help of these estimations, structural model concerning the cryogels in the temperature range of 31-39 ºC (Figure 5) has been created. This model may be also supported by the followed and obtained structural evidences.

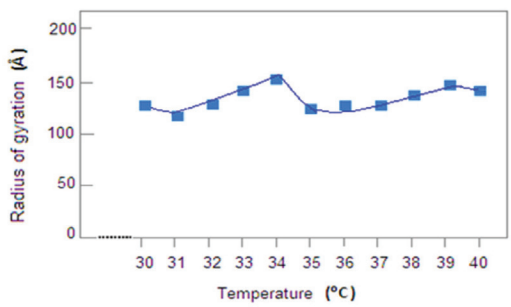

Figure 4. The change of the radius of gyration values (as a measure of the effective pore size filled water) depending on temperature.

The model which is stated in Figure 5 is illustrated as follow. In Figure 5 (a), some of pores are filled water and others are filled with air. When the temperature rises, entire sizes of pores tend to enlarge (b). When it comes to a particular temperature (c), especially the water-filled pores will begin to tear and new water channels will form. As a result of the tear, the water spreads to the environment by finding

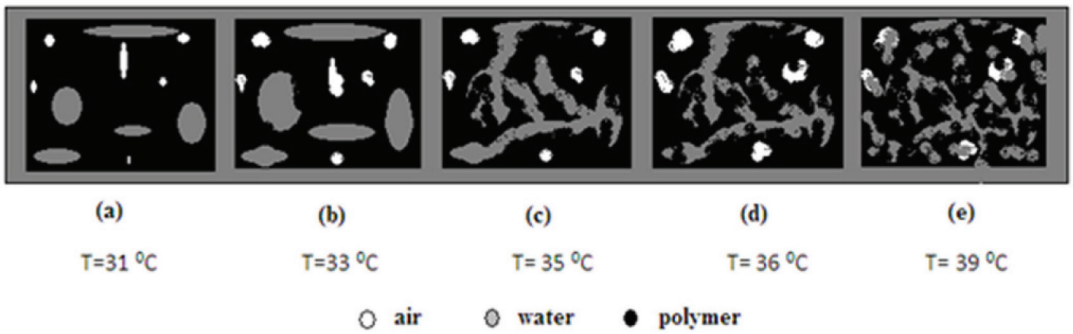

Figure 5. Structural model depending on temperature.

thinner ways and thus shrinkage in the structure appears as a reduction at radius of gyration. Hereafter, when pores filled with water are damaged by temperature increase, crosslinks between these damaged polymer regions might occur. As a result of this cross-linking, new small pores filled with water will occur and pores filled with air will begin to grow by the transport of water through them. The process can be also monitored at higher temperatures. In this study, structural changes tried to be monitored for 30ºC-40ºC temperature range since the aim of this study was to develop advanced biomaterials.

Temperature (T) effect on the poly(NIPA-MAH) cryogels which are in aqueous medium were investigated by recording scattering profiles and evaluation of radius of gyration values of the poly(NIPA-MAH) cryogels in the temperature range of 30ºC-40ºC, ΔT= 1ºC, Δt=15min. Figure 6 and Figure 7 show scattering profiles and radius of gyration values according to the above mentioned temperatures.

Shape of the pores' surfaces can be defined by fractal definitions. When the surface of pores are undergoing fractal roughening, the fractal structure is called a surface fractal. Furthermore, when the surface of pores are smooth, it is called the mass fractal. For fractal objects, it is well known that the scattered intensity I(q) follows a power law, $I(q) \approx q^{-p}$ where p is a fractal dimension. For mass fractals, $1 < p < 3$, while for surface fractals $3 < p < 4$ [37]. The p value is obtained by calculating with drawing curves in Figure 6. p is 1.067 for 34ºC and 1.084 for 35ºC. While temperature increases, the surface fractal dimension is expected to grow resulted from tearing of pores. It may be explained with closed nano pores. As observed in SAXS analysis, increasing temperature do not affect these closed nano pores remarkably. Structural changes of nano pores are less than micro pores. These properties may be appropriate for the reversable usage of the cryogels. For example plant irrigation, skin moisturizer, water holding and quenching, the same amount of water can be given and taken back. The water will not be trapped in the nanopores. But, it is observed that p do not diverse remarkably between 34ºC and 35 ºC. The effect in scattering profiles of structural differences for temperature of 30ºC-35ºC can be seen well from Porod drawing in Figure 7. Structural changes at 34ºC-35ºC critical temperatures can also be recordable easily for the q range of 0.09 – 0.12 $Å^{-1}$ (including the maximums) in the Porod drawing of the scattering data.

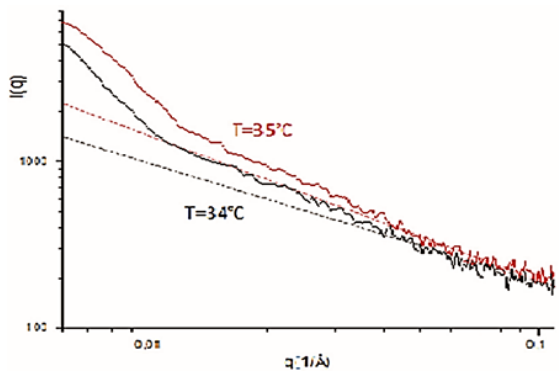

Figure 6. Drawing of the slope for Porod range at 34 ºC and 35 ºC.

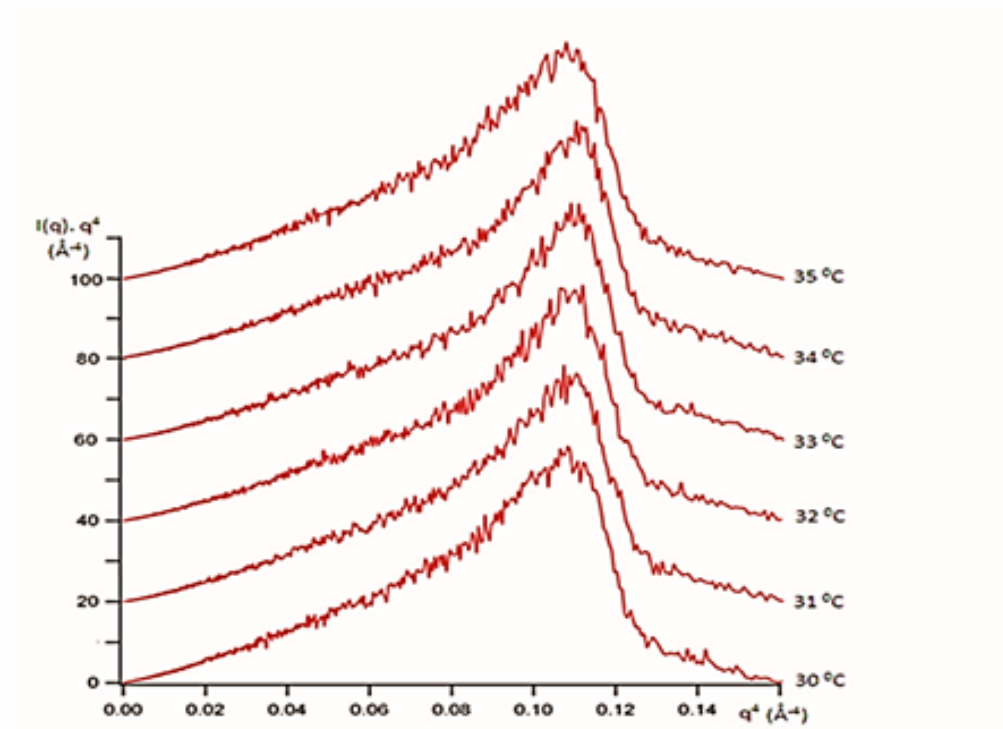

Figure 7. Porod drawings (position of each hump) indicating phase transition at 34ºC-35ºC.

Random coil polymer molecules are expected to be in the content of polymer phase. To explain the X-ray scattering from these type random electron densities, Gaussian chain and the random flight models can be combined. According to this combination, N bonds connected to the polymeric beads (which have higher electron dense regions because of shrinking of the polymeric units or crosslinked gels) in the form of random coils seen in the Figure 8.

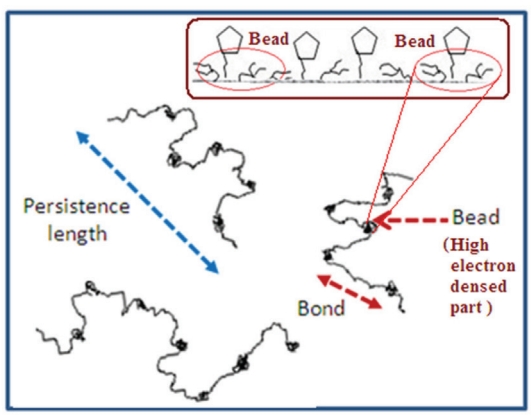

Figure 8. Gaussian chain model for the cryogels including high electron densed parts (beads).

Independent scatterings from random coil polymer molecules can be considered by I(q). q^2 – q graphics for the cryogels at the investigated temperatures. With the help these graphics the persistence lengths can be determined [38, 39]. The persistence length may be defined by a projection of the averaged end-to-end vector onto the first bond direction [40].

The drawing of $I(q).q^2$ versus q (for T=34ºC and 35ºC) have showed that this structural parameters (persistence lengths) are 57.3 and 78.5 Å, respectively (Figure 9). The results related with bigger persistence length and small radius of gyration value (for the pores) of the cryogel at 35ºC have been also supported by bigger scattering volume (Q: invariant).

The area (Q) under the curve of $I(q).q^2$ vs q is proportional to the total scattering volume. Higher temperature causes higher scattering volume. Electron density at 35ºC is also greater than that of 34ºC as expected in the estimated model (Figure 9).

Pore size ienlarges with increasing temperature. When the pores reach a certain critical value, they flatten by tearing and the growth in small pores is observed.

With the help of GNOM program (indirect transform program that evaluates the particle distance distribution function p(r)), pair distance distribution and the expected scattering data fits of the water filled porous structures have been calculated as seen in the Figure 10 [41]. According to these results, it may be said that increasing temperature causes flater polymer walls, higher scattering effect and higher electron densities up to a critical temperature. At the critical temperature pores are starting to rupture. On the other hand big porous structures are dividing into smaller flat and porous aggregations. This may be because of inner cross linking of pore walls by the effect of slight increasing of temperature.

The graphic of I(q) – q for T=34ºC has some peaks in Porod region with respect to the same region for T=35ºC. These peaks may be occured by lamellar aggregation in interface just before rupture of the pores.

The peaks of the graphics in Figure 11 may be defined that different correlation lengths in the horizontal axis D_{max} indicates maximum size of the pores. Zig-zag view or seperate peaks indicate different local electron density distributions and discrete correlation lengths (pair distances). If these discrete peaks show form of a continuous one board and wide distribution, it means that the structure has more uniform electron density localizations. At 35ºC, pores become closer to each other and the pair distances take stable values. So, for 35ºC, the most probable correlation length may be accepted as 300 Å. D_{max} values are equal for these two temperatures. As a measure of electron density and the number of aggregates of the cryogel, the area under the pair distance distribution graphic increase for higher temperature. This observation is convenient to the defined structure model (Figure 12) indicating more polymer parts and higher electron densities in unit volume of the cryogel.

The possibility of anticipating the polymer transition layer thickness in dried and wetted cryogels is another advantage of the SAXS method application in the investigation of polymer-porous materials [42]. To measure transition layer thickness defining the border of two phases (water and polymer), the graphics of the dependence $I(q).q^3$ versus q^2 have been drawn for the phase transition temperatures as seen in the Figure 13.

According to previous reports about the calculation of minimum transition layer thickness,

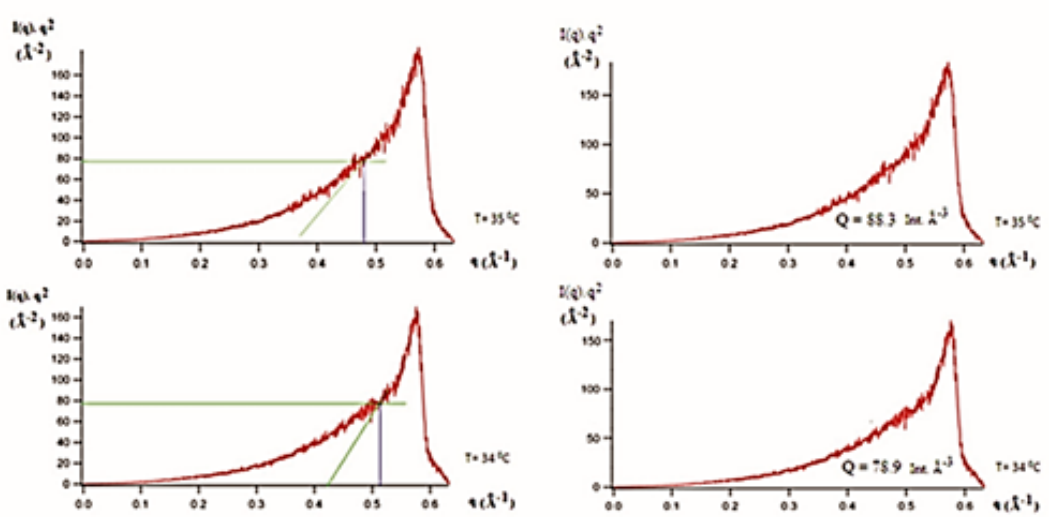

Figure 9. Invariant values indicating a measure of electron densities and determination of persistence lengths at two temperatures

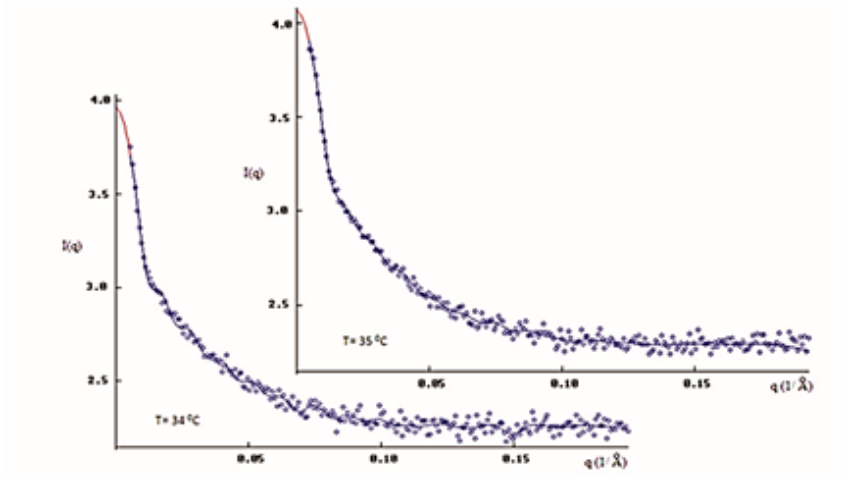

Figure 10. Fit pattern at 34 ve 35ºC temperatures, plotted by GNOM.

the following equation (where c is a constant and E is the transition layer thickness) has been used [42, 43],

$$I(q)q^3 = c\left(1 - \frac{E^2}{6}q^2\right) \qquad (2)$$

This equation has been used for Porod region ($q \to \infty$) of our scattering profiles. The values of E and c have been determined for two cryogels to see the temperature effect on the inner surface of pores by using the slope and intercept values in the graphic of $I(q).q^3$ versus q^2.

As a result of this evaluation in Table 1, it may be said that inner surface area of the polymer borders at T=35ºC is bigger than that of at T=34ºC as expected in the constructed model (Figure 13).

CONCLUSION

Elastic, spongy, porous and mechanically stable (0.8 cm in diameter and 4.0 cm in length) thermosensitive monolithic poly(NIPA-MAH) cryogel was synthesized and characterized. The cryogels are cheap materials and they can be used as reusable materials and also offer great advantages with viscous media. The porous structure of cryogel allows direct processing of whole blood. The porous structures provide rapid response to stimuli besides low flow resistance. When the temperature changed, the properties of the surface of the poly(NIPA-MAH) cryogel

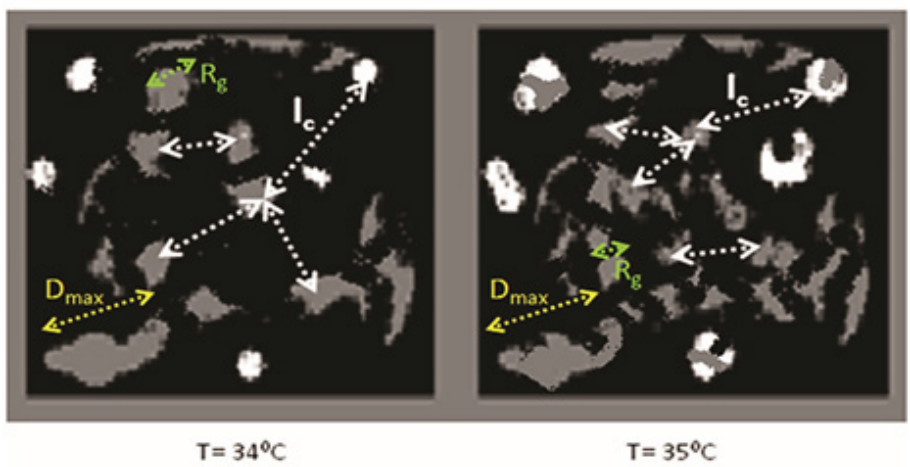

Figure 11. Porous structure model for two temperatures indicating recordable structural change (R_g: radius of gyration, L_c: correlation length, D_{max}: maximum size of the nano aggregations).

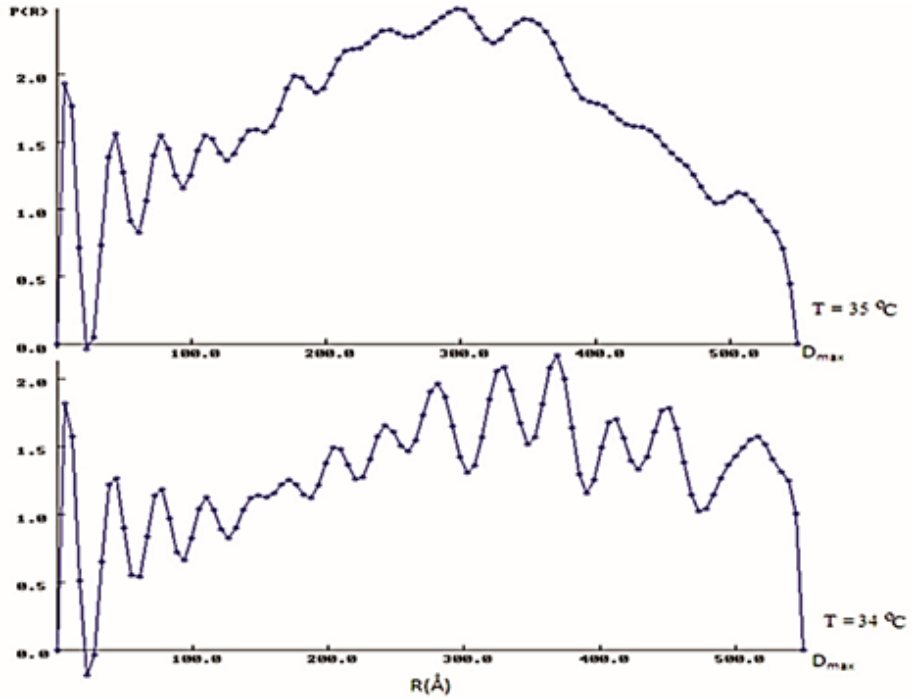

Figure 12. At temperatures of 34 and 35ºC, Pair distance distributions of the nano-aggregats in the cryogels.

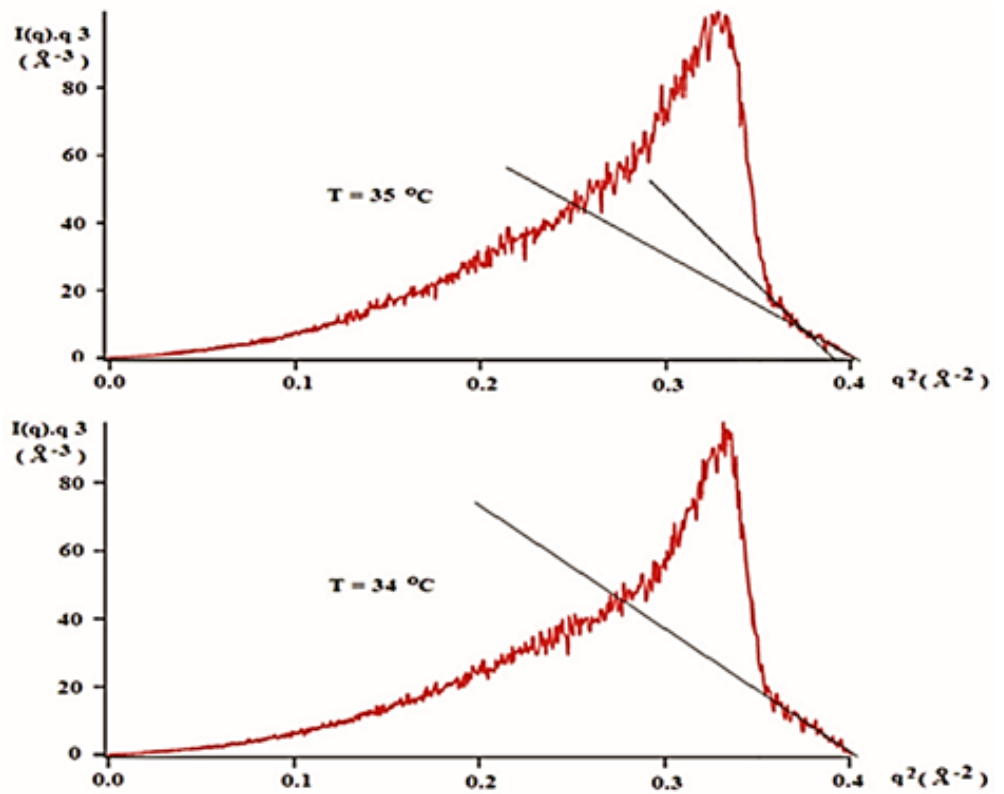

Figure 13. I(q).q^3 versus q^2 graphics for the critical cryogels and the straight lines used to calculate E and c values.

Table 1. Structural parameters obtained from I(q).q^3-q^2 drawings.

Cryogel(in water)	Slope ($Å^{-1}$)	E ^{2} ($Å^2$)	c($Å^{-3}$)
Cryogel at T = 34ºC	343.5	14.8	139.1
Cryogel at T = 35ºC	311.6 484.9	14.8 15.4	126.2 189.1

switched from hydrophilic to hydrophobic. The poly(NIPA-MAH) cryogel present potentially attractive biotecnological materials with adjustable surface properties. It appears that the poly(NIPA-MAH) cryogels can well be applied for the separation and purification of biomolecules and ions. The SAXS experiments give very new series of information about the nanostructural changes induced by temperature in poly(NIPA-MAH) cryogels and also show the wall thickness and pore sizes with increasing temperatures. We expect that our characterization work can help chemists as well as non-chemist to understand the structural changes of thermosensitive and porous cryogels . the thermosensitive polymers have been investigated because of their ease of recovery and their potential for many application [43-46].

ACKNOWLEDGEMENT

SAXS analysis part of the study was supported by a TUBITAK Project : TBAG 113F014.

References

1. A. Kumar, A. Srivastava, I.Y. Galaev, B. Mattiasson, Smart polymers: Physical forms and bioengineering applications, Prog. Polym. Sci., 32 (2007) 1205.
2. E.S. Gil, S.M. Hudson, Stimuli-responsive polymers and their bioconjugates, Prog. Polym. Sci., 29 (2004) 1173.
3. J.R. Zhang, D.K. Misra, Magnetic drug-targeting carrier encapsulated with thermosensitive smart polymer: Core–shell nanoparticle carrier and drug release response, Acta Biomaterialia, 3 (2007) 838.
4. H. Ichikawa, Y. Fukumori, A novel positively thermosensitive controlled-release microcapsule with membrane of nano-sized poly(N-isopropylacrylamide) gel dispersed in ethylcellulose matrix, J. Controlled Release, 63 (2000) 107.
5. A. Kondo, H. Fukuda, Preparation of thermo-sensitive magnetic hydrogel microspheres and application to enzyme immobilization, Journal of Ferment and Bioeng., 84 (1997) 337.
6. A. Kumar, M. Kamihira, I.Y. Galaev, S. Lijima, B. Mattiasson, Binding of Cu(II)-Poly(N-isopropylacrylamide/vinylimidazole) Copolymer to Histidine-Tagged Protein: A Surface Plasmon Resonance Study, Langmuir, 19 (2003) 865.
7. E. Kalaycıoglu, S. Patır, E. Piskin, Poly(NIPA-co-MAH) Copolymers and Their Interactions with Human Immunoglobulin-G, Langmuir, 19 (2003) 9538.
8. H. Tokuyama, T. Iwama, Temperature-Swing Solid-Phase Extraction of Heavy Metals on a Poly(N-isopropylacrylamide) Hydrogel, Langmuir, 23 (2007) 13104.
9. R. Pelton, Temperature-sensitive aqueous microgels, Advances in Coll. and Interf. Sci., 85 (2000) 1.
10. M. Turk, S. Dincer, E. Piskin, Smart and cationic poly(NIPA)/PEI block copolymers as non-viral vectors: in vitro and in vivo transfection studies, J. Tissue Eng. Regen. Med., 1 (2007) 377.
11. N. Shamim, H. Liang, K. Hidajat, M.S. Uddin, Adsorption, desorption, and conformational changes of lysozyme from thermosensitive nanomagnetic particles, J. Coll. and Interf. Sci., 320 (2008) 15.
12. M. Türk, Z.M.O. Rzayev, S.A. Khalilova, Bioengineering functional copolymers. XIV. Synthesis and interaction of poly(N-isopropylacrylamide-co-3,4-dihydro-2H-pyran-alt-maleic anhydride)s with SCLC cancer cells, Bioorg. & Med. Chem., 18 (2010) 7975.
13. K. Nagase, J. Kobayashi, T. Okano, Temperature-responsive intelligent interfaces for biomolecular separation and cell sheet engineering, J.R. Soc. Interface., 6 (2009) 293.
14. N. Bereli, M. Andac, G. Baydemir, R. Say, I. Y. Galaev, A. Denizli, Protein recognition via ion-coordinated molecularly imprinted supermacroporous cryogels, J. Chromatog. A, 1190 (2008) 18.
15. V.I. Lozinsky, I.Y. Galaev, F.M. Plieva, I.N. Savina, H. Jungvid, B. Mattiasson, Polymeric cryogels as promising materials of biotechnological interest, Trends in Biotechnol., 21 (2003) 445.
16. W. Xue, S. Champ, M.B. Huglin, T.G.J. Jones, Rapid swelling and deswelling in cryogels of crosslinked poly(N-isopropylacrylamide-co-acrylic acid), Europ. Polym. Journal., 40 (2004) 703.

17. J. Kobayashi, A. Kikuchi, K. Sakai, T. Okano, Aqueous chromatography utilizing pH-/temperature-responsive polymer stationary phases to separate ionic bioactive compounds, Anal. Chem., 73 (2001) 2027.
18. H. Kanazawa, M. Nishikawa, A. Mizutani, C. Sakamoto, Y. Morita-Murase, Y. Nagata, A. Kikuchi, T. Okanoc, Aqueous chromatographic system for separation of biomolecules using thermoresponsive polymer modified stationary phase, J. Chromatog. A, 1191 (2008) 157.
19. P. Maharjan, W.B. Woonton, E.L. Bennett, W.G. Smithers, K.D. Silva, T.W.M. Hearn, Novel chromatographic separation – The potential of smart polymers, Innov. Food. Sci. and Emerg. Tech., 9 (2008) 232.
20. L. Qin, X.W. He, W. Zhang, Y.W. Li, K.Y. Zhang, Macroporous Thermosensitive Imprinted Hydrogel for Recognition of Protein by Metal Coordinate Interaction, Anal. Chem., 81 (2009) 7206.
21. H. Liu, M. Liu, L. Ma, J. Chen, Thermo- and pH-sensitive comb-type grafted poly(N,N-diethylacrylamide-co-acrylic acid) hydrogels with rapid response behaviors, Euro. Polym. J., 45 (2009) 2060.
22. Y. Liu, X. Cao, M. Luo, Z. Le, W. Xu, Self-assembled micellar nanoparticles of a novel star copolymer for thermo and pH dual-responsive drug release, J. Colloid and Interf. Sci., 329 (2009) 244.
23. E.J. Kim, S. Cho, S.H. Yuk, Polymeric microspheres composed of pH/temperature-sensitive polymer complex, Biomaterials, 22 (2001) 2495.
24. G. Fundueanu, M. Constantin, P. Ascenzi, Preparation and characterization of pH- and temperature-sensitive pullulan microspheres for controlled release of drugs, Biomaterials, 29 (2008) 2767.
25. J.M. Benns, J.S. Choi, R.I. Mahato, J.S. Park, S.W. Kim, pH-Sensitive Cationic Polymer Gene Delivery Vehicle: N-Ac-poly(l-histidine)-graft-poly(l-lysine)Comb Shaped Polymer, Bioconjugate Chem., 11 (2000) 637.
26. H. Yavuz, V. Karakoc, D. Turkmen, R. Say, A. Denizli, Synthesis of cholesterol imprinted polymeric particles, Int. J. Biol. Macromol., 41 (2007) 8.
27. Y. Canak, S. Ozkara, S. Akgol, A. Denizli, Pseudo-specific bioaffinity chromatography of immunoglobulin-G, React. Funct. Polym., 61 (2004) 369.
28. I. W. Hamley, V. Castelletto, M. P. S. N. Ricardo, E.N. M. Pinho, C. Booth, D. Attwood, Z. Yang, A SAXS study of the structure of gels formed by mixtures of polyoxyalkylene triblock copolymers, Polym. Int., 56 (2007) 88.
29. M. H. Zareie, S. Dincer, E. Piskin, Observation of Phase Transition of Thermo-Responsive Poly(NIPA)–PEI Block Copolymers by STM, J. Colloid and Interf. Sci., 251 (2002) 424.
30. M. Chalal, F.E. Dolle, I. Morfin, J.C. Vial, M.R.A. Armas, J.S. Roman, N. Bolgen, E. Piskin, O. Ziane, R. Casalegno, Imaging the Structure of Macroporous Hydrogels by Two-Photon Fluorescence Microscopy, Macromolecules, 42 (2009) 2749.
31. P. Perez, F. Plieva, A. Gallardo, J.S. Roman, M.R. Aguilar, I. Morfin, F.E. Dolle, F. Bley, S. Mikhalovsky, I.Y. Galaev, B. Mattiasson, Bioresorbable and nonresorbable macroporus thermosensitive hydrogels prepared by cryopolymerization. Role of the cross-linking agent, Biomacromol., 9 (2008) 66.
32. H.M. Zareie, E.V. Bulmuş, A.P. Gunning, A.S. Hoffman, E. Piskin, V.J. Morris, Investigation of A Stimuli-Responsive Copolymer by Atomic Force Microscopy, Polymer, 41 (2000) 6723.
33. V. Karakoç, D. Türkmen, H. Shaikh, N. Bereli, C. Andaç, A. Denizli, Synthesis and characterization of Poly(N-isopropyl acrylamide) thermosensitive based cryogel, Hacettepe J. Biol. Chem., 41 (2013) 159.
34. B. Garipcan, A. Denizli, A Novel Affinity Support Material for the Separation of Immunoglobulin G from Human Plasma, Macromol. Biosci., 2 (2002) 135.
35. O. Glatter, O. Kratky, Small Angle X-ray Scattering, Academic Press, London, 1982, p,17
36. R.J. Roe, Methods of X-ray and Neutron Scattering in Polymer Science, Oxford Univ. Press., 2000, 184- 185
37. A. Owen, A. Bergmann, On the fractal character of polymer spherulites: an ultra-small-angle X-ray scattering study of poly[(R)-3-hydroxybutyrate] , Polym. Int., 53 (2004) 12.
38. O. Kratky, G. Porod, Diffuse small-angle scattering of X-rays in colloid systems, J. Coll. Interf. Sci., 4 (1949) 35
39. O. Kratky, G. Porod, Röntgenuntersuchung gelöster Fadenmoleküle, Rec. Trav. Chim., 68 (1949) 1106
40. R.J. Roe, Methods of X-ray and Neutron Scattering in Polymer Science, 2000, p. 166
41. D.I. Svergun, Determination of the regularization parameter in indirect-transform methods using perceptual criteria, J. Appl. Crystallogr., 25 (1992) 495.
42. S. Pikus, A.L. Davidowicz, E. Kobylas, D. Wianowska D, SAXS examination of the water evaporation process from silica materials coated with a polysaccharide–polyimine copolymer layer, Appl. Surf. Sci., 156 (2000) 189.
43. S.A. Ravion, Z. Ding, A. Pelle, A.S. Hoffman, D. Letourneur, New antibody purification procedure using a thermally responsive poly(N-isopropylacrylamide)-dextran derivative conjugate, J. Chromatogr. B, 761 (2001) 247.

44. N. Malmstadt, P. Yager, A.S. Hoffman, P.S. Stayton, A Smart Microfluidic Affinity Chromatography Matrix Composed of Poly(N-isopropylacrylamide)-Coated Beads, Anal. Chem., 75 (2003) 2943.
45. R. B. Fong, Z. Ding, A. S. Hoffman, P. S. Stayton, Affinity Separation Using an Fv Antibody Fragment-"Smart" Polymer Conjugate, Biotech. and Bioengineering., 79 (2002) 271.
46. Z. Xu, W. Bae, A. Mulchandani, R. K. Mehra, W. Chen, Heavy Metal Removal by Novel CBD-EC20 Sorbents Immobilized on Cellulose, Biomacromolecules, 3 (2002) 462.